Surface modifications during femtosecond laser ablation in vacuum, air and water

S. Besner, J.-Y. Degorce, A. V. Kabashin, M. Meunier*,
Laser Processing Laboratory, Department of Engineering Physics, École Polytechnique de Montréal, Case Postale 6079, succ. Centre-ville, Montréal (Québec), H3C 3A7, Canada

ABSTRACT

Femtosecond laser ablation technique has been used to process Si and Au targets in vacuum, air and water environment. The threshold of ablation was found to be much lower for Si compared to Au and that was related to much better radiation absorption of Si. The values of the threshold were almost identical for vacuum, air and water in the case of Si (0.4 J/cm^2 0.2 J/cm^2 in the single and multi-pulse irradiation regime, respectively) and Au (0.9 J/cm^2 and 0.3 J/cm^2). Craters on the surface of Si and Au were essentially similar for low fluences, suggesting an involvement of the same radiation-related mechanism of material removal, whereas for high fluences significant differences could take place. In particular, quite different crater morphologies were observed during the laser ablation in water, including ones with nanoporous layers for Si and ones with concentric spheres for Au. The differences of morphologies for high laser fluences were explained by the involvement of plasma-related effects under the processing in relatively dense media.

Keywords: laser ablation, silicon, gold, surface modifications

1. INTRODUCTION

Due to a significant reduction or complete removal of heat-affected zone (HAZ) as a direct consequence of the pulse being much shorter than the phonon-related heat diffusion time, the femtosecond laser technique manifested itself as a very efficient tool for micromachining applications [1]. The reduction of the HAZ leads to much sharper contours of the laser-processed structures compared to the nanosecond ablation case and, as a consequence, to much better quality of surface processing [1,2]. Generally, the femtosecond laser-based micromachining is performed at relatively low laser fluences and under reduced ambient pressures (in vacuum) to exclude or minimize the impact of plasma effects that can lead to undesirable secondary treatment of the target and consequent deterioration of the processing quality [3,4].

However, some applications require the maximization of laser intensity and operation in dense environments. One of prominent examples is the air optical breakdown processing of semiconductors [5-7], which consists in the use of hot laser generated plasma, produced in an atmospheric pressure gas, to treat surfaces. Another example is the laser ablation of solid targets in liquid environments to fabricate colloidal nanoparticles [8-15]. These experiments are characterized by the presence of hot plasma, capable of both ablating the target and heating the ablated material. In spite of the existence of few papers on the analysis of target surface in these conditions [14,16], properties of laser ablation in different environments have not yet been systematically studied.

In this paper, we compare morphological properties of structures, formed by femtosecond laser ablation of silicon and gold, in three different environments: vacuum, air and water.

2. EXPERIMENAL SETUP

The femtosecond laser radiation from an amplified Ti:Sapphire laser system (λ=800nm, 170 fs, 1kHz) was used to ablate a fresh silicon (100) wafer and a gold disc target. The gold disk was mechanically polished prior to a laser treatment. The laser beam was focused by an objective with a focal length of 7cm and the laser fluence was controlled

* michel.meunier@polymtl.ca; École Polytechnique de Montréal, Laser processing Laboratory, Département de Génie Physique, Case Postale 6079, succ. Centre-ville, Montréal (Québec), Canada, H3C 3A7

Photonics North 2004: Photonic Applications in Astronomy, Biomedicine, Imaging, Materials Processing, and Education, edited by J. C. Armitage, R. A. Lessard, G. A. Lampropoulos, Proc. of SPIE Vol. 5578 (SPIE, Bellingham, WA, 2004) · 0277-786X/04/$15 · doi: 10.1117/12.567746

by changing the radiation energy. The target was place inside a chamber, mounted on an x-y-z translation stage with submicron precision of the target positioning (detailed description of the laser microfabrication system is given in Ref. 17). The experiments were carried out in air, water and vacuum ($6.3x10^{-3}$ mbar). For water tests, the sample was placed in a vessel filled with distilled water. A large surface-to-depth ratio vessel was used to minimize meniscus effects on focusing. The thickness of water above the target surface was 10 mm. The surface morphology was examined by optical microscopy (OM) and scanning electron microscopy (SEM).

To correctly estimate absolute values of the laser fluence in our conditions, we measured the beam waist (diameter of the spot corresponding to $1/e^2$ decrease of the radiation intensity) in the focal plane of the focusing objective. For this purpose, we used the "knife edge" technique, in which a Si blade-based knife was progressively moved over the focal plane of the laser beam, blocking some of its radiation power, while the power of the passed beam was recorded behind the focal plane by a photodetector (Ophir Nova PD-300) [18]. For a correct comparison of ablation parameters for three different ambient media, we determined the precise location of the focal plane for every medium. The focusing objective was displaced over the optical axis of the system (z-axis), while produced craters on Si and gold were examined by SEM. All tests were done at relatively low laser energies, near the ablation threshold to avoid breakdown and filamentation phenomena, which could affect the crater profiles. The point corresponding to the focal plane was determined by finding the lens position providing the smallest diameter of formed craters on the target. It was found that the focal plane is much farer for water when compared to vacuum and air. This phenomenon was apparently related to the shift of the focal point toward the region behind the target due to the refraction of the radiation by water (n_{water} = 1.33 compared to n = 1 for vacuum and air). The point z = 0 will be referred as the focal plane for both vacuum (air) and water, although the absolute focal point values are different for these media.

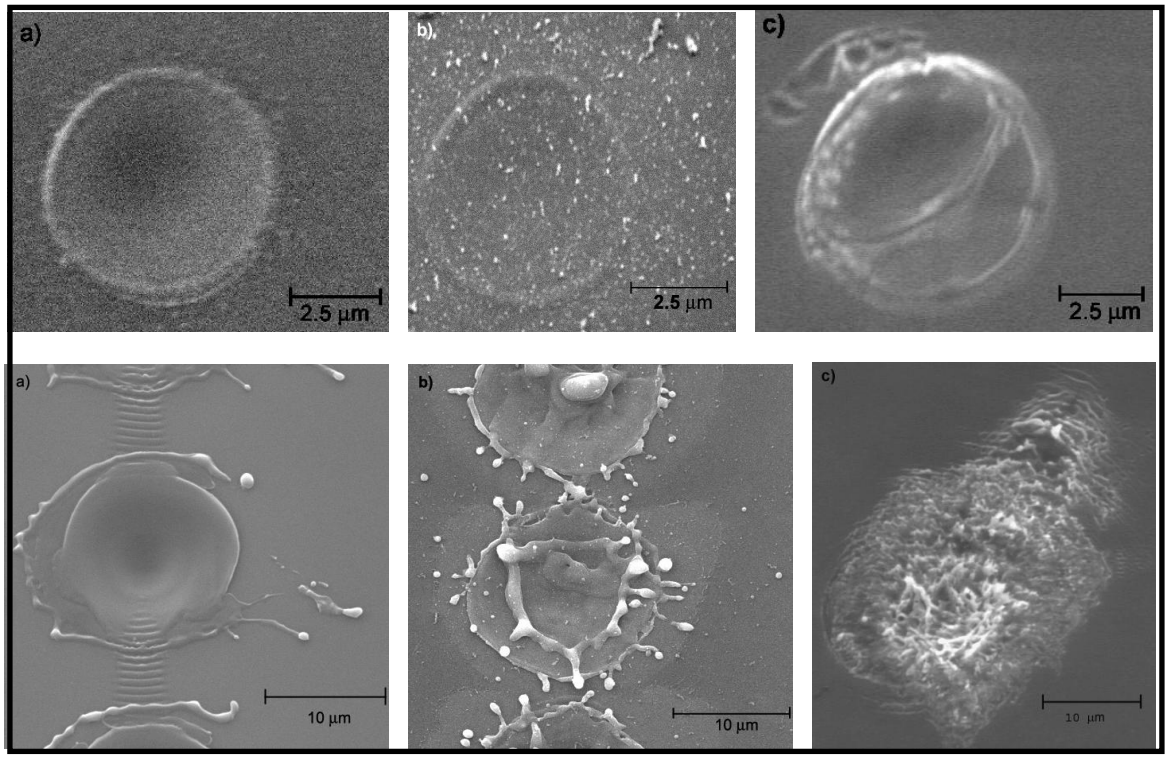

Figure 1: SEM images of craters on Si surface after its ablation by a single fs pulse at low (F~1 J/cm^2, upper images) and high (F~20 J/cm^2) fluences in Vacuum (a), Air (b) and water (c). For water, the data are given for 4 pulses.

3. RESULTS AND DISCUSSION

3.1. Ablation of silicon

As shown on figure 1, for low fluences craters were circular and had almost identical shape and diameter for vacuum, air and water, suggesting that the medium did not affect the ablation process. However, the morphological structures of the laser process surface were quite different as fluence increase. For vacuum, the craters were relatively smooth structures, very similar for low and high fluences. For air, we additionally saw splashes and signs of surface erosion, as shown in Fig. 1b. For water, we observed quite different structures with high aspect ratio columns, ripples and significant increase of the modified surface area [Fig. 1c]. The formation of such structures could be explained by an involvement of additional factors related to the production of plasma or a collapse of the cavitation bubble [19].

By examining a linear region of the fluence dependence for the diameter squared of the ablated surface, we were able to determine thresholds of the material ablation in different media. The ablation threshold was found to depend on the number of pulses used for the ablation, while the thresholds were similar for the three tested media. For 10 pulses (N = 10), the values of the threshold fluence were $F_{vacuum} = 0.2\pm0.07$ J/cm^2, $F_{air} = 0.26\pm0.05$ J/cm^2 and $F_{water} = 0.2\pm0.03$ J/cm^2 for vacuum, air and water respectively, whereas the relevant values for the single pulse regimes were slightly higher: $F_{vacuum} = 0.38\pm0.09$ J/cm^2, $F_{air} = 0.41\pm0.04$ J/cm^2 (the determination of the ablation threshold for water was difficult in the single pulse regime).

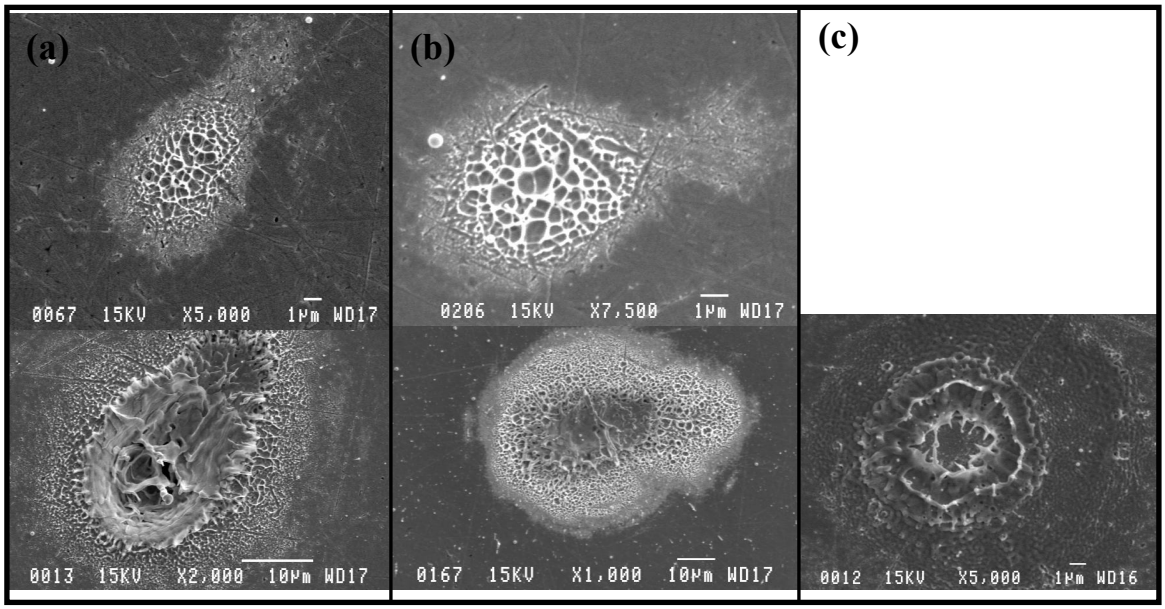

Figure 2: SEM images of craters on the gold surface after its ablation by single fs pulse at low (F~1 J/cm^2, upper images) and high (F~500 J/cm^2, lower images) fluences in Vacuum (a), Air (b) and water (c)

3.2. Ablation of gold

First, we found that the ablation of gold takes place at much higher laser fluences. This is apparently explained by a weaker absorption ($R_{Au} \sim 0.95$ and $R_{Si} \sim 0.35$ at 800nm) of radiation by gold compared to Si. The craters on the gold surface were also essentially different compared to the case of silicon. Fig. 2 shows typical craters on gold after its ablation by a single laser pulse in three different media. One can see that under low fluences (F < 10 J/cm^2) morphologies of craters produced in vacuum and air were almost identical. Here, a very porous central region surrounded by a surface-eroded halo can be seen. These modifications are consistent with the phase explosion as the mechanism of material removal during the femtosecond laser ablation [1]. Note that for water no visible modifications could be seen at low fluences. For high fluences, craters became much deeper in the case of vacuum [Fig. 2a] compared to air [Fig. 2b]. This was probably related to much lower laser intensity on the target surface in the case of air as a result of air breakdown phenomena, leading to energy losses before the target [3]. For water, the craters were quite

different with concentric circular structures, as shown in Fig. 1c. The distance between the circular structures was of the μm scale and depended on the laser fluence. The nature of these structures is not yet clear. However, we reason that it can be related to the collapse of the cavitation bubble. This bubble is formed as a result of the energy transfer from the plasma to the nearby liquid layer, leading to the vaporization of water [19]. The bubble collapses 100 to 200 μs after the laser pulse, releasing a significant amount of mechanical energy. Such energy can be sufficient to cause a secondary cavitation-based ablation of material from the target surface in water yielding to an explosion-like character of craters.

As in the case of Si, the fluence dependence of the squared diameter of the ablated area was characterized by the presence of a linear regime at low fluences. Examining this linear region, we can determine ablation thresholds of gold in three media. In the single pulse regime, these thresholds were almost similar for vacuum and air (0.95±0.05 J/cm^2 and 0.92±0.1 J/cm^2, respectively). In the multi pulse regime, the values of the threshold were much lower (0.34±0.06 J/cm^2, 0.33±0.1 J/cm^2 and 0.25±0.07 J/cm^2 for vacuum, air and water, respectively). The decrease of the threshold in the multi pulse regime was apparently connected to better absorption of radiation due to the appearance of rippled surface relief after its irradiation.

4. CONCLUSION

In summary, we carried out an empiric study of surface modifications during femtosecond laser ablation of gold and silicon in vacuum, air and water. We showed that the thresholds of material ablation and the shape of craters at low laser fluences were similar for three media, suggesting a medium-independent mechanism of material ablation in those conditions. In contrast, the ablation at high fluences was characterized by rather different shapes and structures of formed craters for these three media. The difference was related to an involvement of plasma phenomena in relatively dense media, which could lead to an additional material ablation or surface modifications.

5. REFERENCES

1. J. F. Ready, D. F. Farson, *LIA Handbook of Laser Materials Processing* (Springer-Verlag and Heidelberg GmbH & Co.: Berlin, 2001).

2. B. N. Chichkov, C. Momma, S. Nolte, F. Von Alvensleben, A. Tunnermann, Appl. Phys. A., **63** (1996) 109.

3. C. Momma, S. Nolte, G. Kamlage, F. Von Alvensleben, A. Tunnermann, Appl. Phys. A., **67** (1998) 517.

4. S. M. Klimentov, T. V. Kononenko, P. A. Pivovarov, S. V. Garnov, V. I. Konov, A. M. Prokhorov, D. Breitling, and F. Dausinger, Quantum Electron. **31** (2001) 378.

5. A.V. Kabashin, M. Meunier, *Appl. Phys. Lett.,* **82** (2003) 1619.

6. A.V. Kabashin, M. Meunier *Mat. Sci. Eng. B*, **101** (2003) 60.

7. D.-Q. Yang, A. V. Kabashin, V.-G. Pilon-Marien, E. Sacher and M. Meunier, J. Appl. Phys. **95** (2004) 5722.

8. A. Fojtik, and A. Henglein, Ber. Bunsen-Ges. Phys. Chem. **97** (1993) 252.

9. F. Mafune, J-Y. Kohno, Y. Takeda, T. Kondow, and H. Sawabe, J. Phys. Chem., B, **104** (2000) 9111.

10. Y.-H. Chen, and C.-S. Yeh, Colloids & Surfaces, **197** (2002) 133.

11. S. I. Dolgaev, A. V. Simakin, V. V. Voronov, G. A. Shafeev, and F. Bozon-Verduraz, Appl. Surf. Sci. **186** (2002) 546.

12. T. Tsuji, K. Iryo, N. Watanabe, and M. Tsuji Appl. Surf. Sci. **202** (2002) 80.

13. A. V. Kabashin, M. Meunier, K. Kingston, and J. H. T. Luong J. Phys. Chem. B **107** (2003) 4527.

14. A.V. Kabashin, M. Meunier *J. Appl. Phys.* **94** (2003) 7941.

15. J.-P. Sylvestre, A.V. Kabashin, E. Sacher, M. Meunier, J.H.T. Luong *J. Am. Chem. Soc.*, **126** (2004) 7176.

16. G. Daminelli, J. Kruger, W. Kautek, Thin Solid Films, 467 (2004) 334.

17. M. Meunier, B. Fisette, A. Houle, A.V. Kabashin, S. V. Broude, and P. Miller, Proc. SPIE, **4978** (2003) 169.
18. S. Besner, J.-Y. Degorce, A. V. Kabashin, M. Meunier, Appl. Surf. Sci., in press (2004).
19. A. Vogel, J. Noack, K. Nahen, D. Theisen, S. Busch, U. Parlitz, D.X. Hammer, G.D. Noojin, B.A. Rockwell, R. Birngruber, Appl. Phys. B, **68** (1999) 271.